Letter

Frequency and spatially chirped free-electron laser pulses

S. Reiche,[1,*] C. Bacellar,[2] P. Bougiatioti,[2] C. Cirelli,[2] P. Dijkstal,[1,†] E. Ferrari,[1,†] P. Juranić,[1] G. Knopp,[2] A. Malyzhenkov,[1,‡] C. Milne,[2,§] K. Nass,[2] E. Prat,[1] J. Vila-Comamala,[2] and C. David[2]

[1]*GFA, Paul Scherrer Institute, CH-5232 Villigen PSI, Switzerland*

[2]*PSD, Paul Scherrer Institute, CH-5232 Villigen PSI, Switzerland*

(Received 13 May 2022; accepted 22 February 2023; published 10 April 2023)

We have produced hard x-ray free-electron laser (FEL) pulses, which are chirped both in photon energy and in spatial position. The experiments have been carried out at the hard x-ray beamline Aramis at SwissFEL, located at the Paul Scherrer Institute in Switzerland. The FEL beamline was operated without any external focusing and with a tilted, energy-chirped electron bunch, whose properties are then transferred to the photon beam. The resulting FEL pulses were used for a single-shot absorption x-ray spectroscopy experiment at the Alvra endstation. But, as will be outlined, applications of this type of tailored FEL pulse go beyond such experiments, allowing for x-ray pulse compression and control of the transverse coherence within the pulse.

DOI: 10.1103/PhysRevResearch.5.L022009

With the realization of hard x-ray free-electron lasers (FELs) worldwide [1–5] coherent light sources became available for studies in fields related to material science, chemistry, biology, and beyond.

The basic principle of the exponential amplification of spontaneous undulator radiation, the self-amplified spontaneous emission (SASE) process [6,7], increases the emitted radiation by several orders of magnitude. While the transverse coherence of the process almost reaches its maximum, the longitudinal coherence is limited. Although the relative width of the SASE spectrum, below 0.1%, may be considered small, it still exhibits many spikes and fluctuates from shot to shot due to the underlying unstable seed signal of the incoherent spontaneous radiation [8].

Some classes of user experiments benefit from an increased spectral bandwidth of the FEL signal, in particular x-ray crystallography [9–12], x-ray emission and absorption spectroscopy [13], stimulated Raman spectroscopy [10], and multiple wavelength anomalous diffraction [14]. There is also an operational benefit if the spectrum covers the entire photon energy range of interest: the desired photon energy can be selected with a monochromator while keeping the machine part of the FEL unchanged.

Most of the user experiments requiring high resolution of the spectral content, like x-ray absorption spectroscopy, scan a monochromator to measure the absorption curve. This is time consuming since it requires a reference measurement without the sample and sufficient statistics since a filtered SASE signal is prone to large pulse energy fluctuations [8]. Thus it takes many shots per monochromator setting to overcome the stochastic error in the measurement. These classes of experiments become more efficient if the FEL pulse is split by a zone plate [15] and then dispersed in frequency in the perpendicular plane [16], thereby providing all information in a single shot. Only one of the split pulses interacts with the sample. The basic idea, presented here, is to provide a frequency-dispersed FEL pulse already from its undulator source. This avoids the optical element, which disperses the FEL signal but might also reduce the spectral intensity—namely in the soft x-ray regime. Secondly, the dispersed signal is available at all user stations, offering more versatility to single shot spectrally resolved experiments.

We report on the demonstration of a spatially tilted, frequency-chirped FEL pulse. It was realized at the hard x-ray beamline Aramis at SwissFEL [17] in conjunction with a user experiment at the Alvra endstation following the experimental methods of dispersive x-ray absorption spectroscopy [18–21] but without the need of the dispersive element at the user endstation. Our report will focus exclusively on the machine-side implementation of this mode, leaving the discussion and results of the user experiments to a separate publication. Besides single-shot spectroscopy there are additional applications of such spatially and frequency chirped pulses, such as FEL pulse compression [22] or transverse coherence control, to avoid speckle noise in coherent diffraction experiments with noncrystalline samples [23]. We will get back to this towards the end of this Letter.

Our approach to implement this special operation mode combines three elements, described in the following: (1) the generation of a correlated energy chirp along the bunch, (2) the formation of a spatial tilt of the beam by means of leaking dispersion, and (3) the propagation through the undulator without any focusing to guarantee that both transverse and energy chirps of the electron beam are imprinted on the FEL

*sven.reiche@psi.ch

†Present Address: Deutsches Elektronen-Synchrotron, D-22607 Hamburg, Germany.

‡Present Address: CERN, CH-1211 Geneva 23, Switzerland.

§Present Address: European XFEL, D-22869 Schenefeld, Germany.

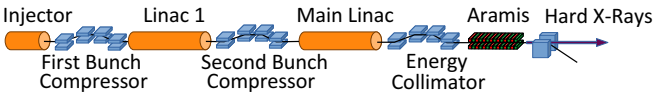

FIG. 1. Schematics of the Aramis beamline at SwissFEL.

pulse. Each of these elements had been demonstrated individually, in particular the demonstration of a large bandwidth by means of overcompression in the second bunch compressor [24] and the slicing of the FEL pulse by means of leaked dispersion [25]. The work, presented here, goes beyond those works by adding a nonoscillating beam tilt in the undulator beamline and by operating the hard x-ray FEL beamline Aramis without any external focusing. Note that a similar idea has been proposed for the soft x-ray beamline Athos at SwissFEL [26], where the requirement of a chirped energy electron bunch is replaced or supplemented by a transverse gradient undulator field of the undulator modules [27].

Figure 1 shows a schematic layout of the SwissFEL facility. The photoelectron gun produces bunches with 200 pC charge and 20 A peak current at a repetition rate of 100 Hz. The bunch length is then reduced in two magnetic chicanes (bunch compressors) at 300 MeV and 2.2 GeV. For the hard x-ray beamline Aramis, the main linac tunes the bunch energy between 3 and 6 GeV, resulting in resonant photon energies of the FEL between 2 and 12 keV. An energy collimator protects the undulator against failure of rf stations as well as from irradiation by bremsstrahlung from the main linac. Its configuration plays a significant role in the demonstration of the spatially tilted beam.

The first step to produce a spatially tilted FEL pulse consists in generating the energy chirp in the electron beam. In normal operation, the run-time differences in a magnetic chicane compress the bunch if the beam is injected with an energy chirp along the bunch with lower-energy particles entering first. At SwissFEL the residual chirp after the second bunch compressor, with a root-mean-square (rms) width of 0.56% at about 2.2 GeV, is subsequently removed by the wakefields of the accelerating rf structures [28] of the main linac. For our purpose we increase the initial chirp at the last compression stage, so that the bunch is overcompressed, to yield the same peak current value of about 2 kA but with opposite energy chirp, where higher energetic particles leave the magnetic chicane first. In this configuration the wakefields increase the chirp, roughly doubling the absolute variation of energy along the bunch at the undulator entrance. At a final energy of 5.5 GeV the rms energy spread of the bunch amounts to about 0.42% (23 MeV), when injected into the undulator beamline. In the process of overcompression, the electron bunch briefly goes through maximum compression. This point is placed between the third and fourth dipole of the magnetic chicane to avoid strong effects from coherent synchrotron radiation (CSR) [29], otherwise destroying the electron beam quality. In fact overcompression also removes the horn structure in the current profile [24], typical for standard compression configuration, and overall the current distribution is smoother, similar to a Gaussian distribution. Not all parts of the electron bunch will contribute to the chirped FEL pulse, since in the head and tail of the bunch the beam current is too low to reach saturation within the length of the undulator. This causes an effective cut in the achievable photon energy chirp. The utility of wakefields to achieve such a large energy chirp is most pronounced at SwissFEL owing to the stronger wakefields in the accelerating structures and the lowest beam energy when compared to other hard x-ray facilities. The chirp could further be enhanced by lowering the path length dependence of the last bunch compressor, expressed by the R_{56} value, and by additional wakefields from passive structures [30].

The second step entails tilting the electron bunch horizontally for the injection into the undulator beamline. Several methods are available, like transverse deflecting structures [31,32], transverse wakefields from passive structures [33], or dispersion with an energy-chirped electron bunch [25,34]. Since the beam has a large energy chirp, leaking dispersion is the most suitable approach. This avoids the instability from phase jitters in rf deflecting structures or the nonlinear tilt generated with the transverse wakefields of passive structures [35]. The beam transport is configured so that the tilt has its maximum spatial extent at the undulator entrance, which is then preserved during the FEL interaction, as discussed in the next paragraph. The leak is generated in the Aramis energy collimator of SwissFEL, a magnetic chicane similar to the bunch compressors, but with strong quadrupole magnets bending back the dispersion function so that there is no energy dependence on the time of flight through the energy collimator. For the nominal isochronous configuration six quadrupoles provide sufficient control of the dispersion function as shown in the upper plot of Fig. 2 (the collimator is located between $z = 440$ m and $z = 461$ m). Modifying the strength of the fourth and sixth quadrupole allows for a dispersion leakage with the least disruption of the optical Twiss functions. Quadrupoles between the energy collimator and the undulator provide the matching of the beam at the undulator entrance and the right betatron phase advance $\Delta\phi$, which has to fulfill the condition $|\sin(\Delta\phi)| \approx 1$. We measured the dispersion for the configuration of a 4 cm dispersion function value along the undulator to verify the setup. The measured dispersion (green dots) does not match the theoretical prediction very well (blue line) and diverges over the undulator beamline, located between $z = 475$ m and $z = 565$ m. However, a postexperiment analysis explains this with an error in the assumed energy of the electron beam. Adjusting all quadrupoles by just 0.2% in strength gives a reasonable agreement of the model with the measurements (orange line in the plot). Systematic errors of each measurement point arise from the calibration uncertainty of the beam position monitor readings, which can be up to 20% for large amplitudes. For the measurement of the spatially tilted FEL beam, optics settings for the mentioned 4 cm dispersion as well as for 10 and 20 cm have been provided to control the spatial size of the tilt. The impact of an energy error on the optics is shown in the lower plot of Fig. 2. The deviation is up to 2 m for betatron values of around 40 m at the undulator beamline location. It should not have any significant impact on the FEL performance.

The third step deals with transporting the electron beam without focusing in the undulator beamline to preserve the tilt orientation. Otherwise the tilt would oscillate, suppressing the FEL amplification. (Parts of the beam that are not aligned to

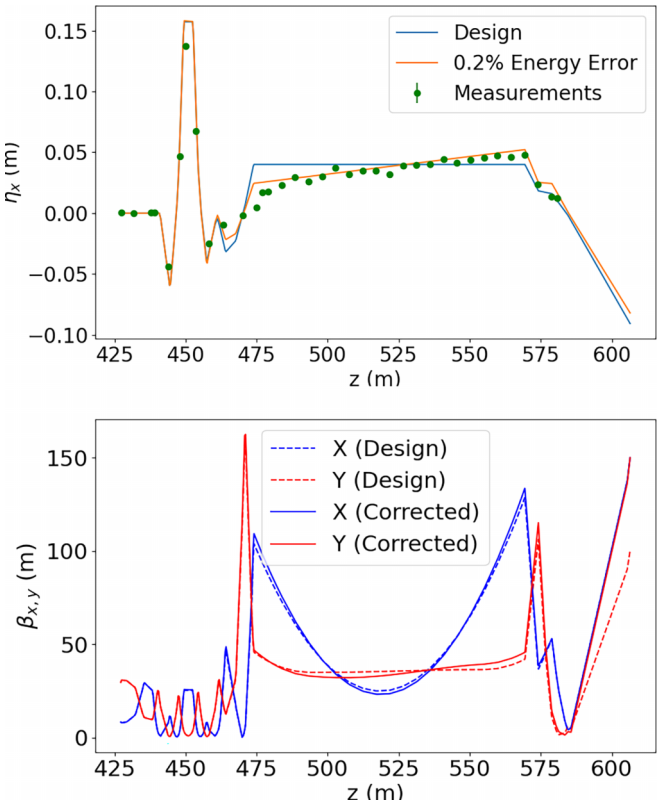

FIG. 2. Upper plot: leaked dispersion from the energy collimator through the undulator beamline. Green circles indicate dispersion measurements at available beam position monitors, while the blue line marks the design optics for the dispersion function. Adjusting the beam energy in the beamline for an unknown systematic shift in the beam energy measurement results in the orange prediction (best fit to the measurement data). Lower plot: Twiss parameters β_x and β_y along the Aramis undulator line (blue and red, respectively). The design optics are drawn with a dashed line, while the solid lines include the energy error of 0.2% in all magnets.

the undulator axis will not experience FEL gain, which results in a reduction of the photon pulse length.) The penalty for operating an FEL without focusing is the reduced electron density and thus a reduced gain. For SwissFEL the average Twiss β function increases from a mean value of 10 m to about 40 m in both planes. Simulations with Genesis 1.3 [36] show a drop of the FEL pulse energy by 30% at a photon energy of 8.5 keV, while the saturation length increases from 32 m to 41 m. Both cases saturate within the given length of the Aramis undulator and the drop in pulse energy in one case is tolerable. This has also been verified experimentally by turning off the focusing in preparation for the setup but disabling the generation of the tilt. Here, the pulse energy dropped from 300 μJ to 200 μJ. Even though the numbers are very similar in experiment and simulation, the experimental setup was not fully optimized for best performance, mainly due to lack of time. Thus even better performance could be expected with more time for optimization. When the tilt is applied, the pulse energy drops only by a few percent for the 4 and 10 cm dispersion cases, but significantly more for 20 cm.

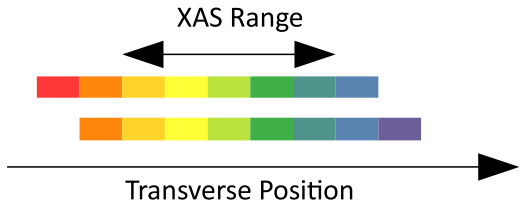

FIG. 3. Exemplary impact of mean electron energy jitter for two shots in the spectral-spatial distribution of the FEL pulse. As long as the region of interest for x-ray absorption spectroscopy (XAS) lies within each bandwidth of each pulse there is an active stabilization of the position for a given photon energy.

Leaked dispersion makes the electron bunch orbit sensitive to mean energy jitter and consequently causes a jitter in the mean position of the FEL pulse. However, the dispersion defines the orbit for a given electron energy deviation independent of its cause, which can be a combination of the bunch mean energy, the longitudinal position along the energy chirped bunch and within the distribution of the uncorrelated slice energy spread. The same idea for "sorting" the orbit with leaked dispersion has been used in the proposal to overcome large energy spread in laser-plasma driven accelerators [37]. Figure 3 illustrates the impact of energy jitter on the observed FEL pulse. While the envelope jitters with the electron bunch energy, the frequency components are stabilized for the single-shot x-ray absorption spectroscopy experiment. For SwissFEL the relative energy jitter is typically below 2×10^{-4}, which corresponds to an orbit jitter of up to 20 μm for the case of 10 cm dispersion within the undulator. This is less than 10% of the total streaked rms beam size of several hundreds of micrometers. Compared to the other available method at SwissFEL of generating a beam tilt, the C-band transverse deflector has a phase error of 0.036°. This corresponds to an effective arrival jitter of about 20 fs and thus comparable to the rms bunch duration. As a result, the orbit jitter would be similar to the rms size of the streaked beam, much more than when the streaking is done with dispersion.

Since the tilt induces a significant horizontal beam size in the millimeter range (e.g., an rms width of 500 μm for the 10 cm dispersion case), a planar undulator type such as in Aramis is favorable since its good-field region is sufficiently large to accept the spatial extent of the tilted electron beam [38]. In addition, the residual focusing, also called natural focusing of the undulator [39], occurs for this undulator type only in one plane, which in our case is the vertical plane. The applied tilt must be perpendicular to preserve it along the undulator.

We have measured the FEL transverse properties with a YAG screen 31 m downstream of the undulator exit, as displayed in Fig. 4. Due to diffraction the individual modes of the FEL appear larger on the observed screen. However, this divergence is still small enough such that the spatial extent still dominates.

With the optics settings for 10 cm dispersion function the observed full-width extension of the x-ray pulse 31 m downstream of the undulator is about 2 mm. Due to the energy error in the quadrupole strength the dispersion grows with distance. The associated divergence of the electron beam is transferred

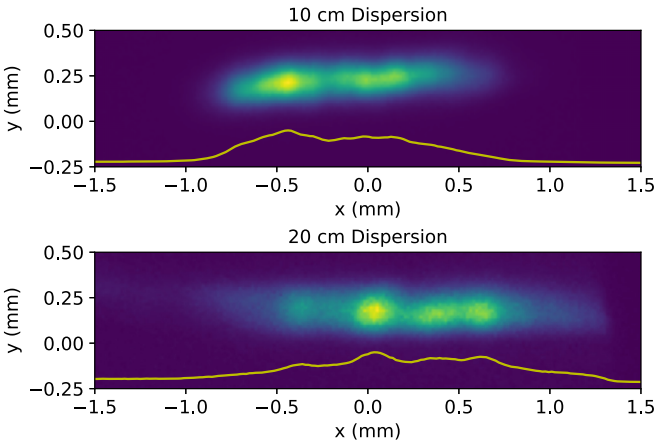

FIG. 4. Direct imaging of the FEL pulse, 31 m downstream of the undulator exit for 10 (top) and 20 cm dispersion (bottom).

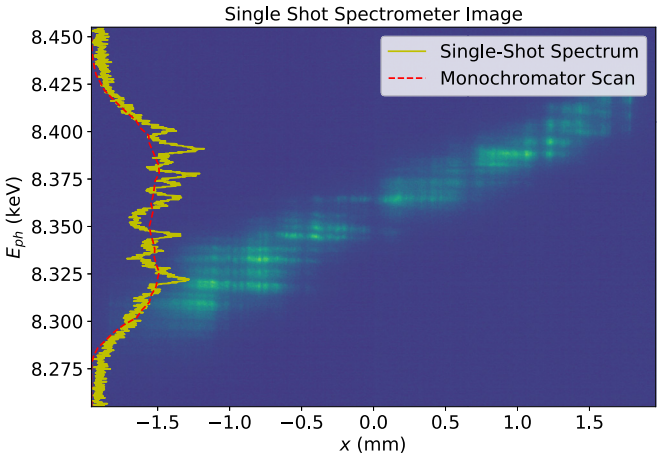

FIG. 5. Spectrometer image obtained with a bent crystal, showing a strong correlation between horizontal position (horizontal axis) and photon pulse energy (dispersion on vertical axis). The projection shows the single-shot spectral measurement (yellow) and the monochromator scan results for calibrating the y axis (red).

to the photon beam. With an extrapolation from the measured electron dispersion (Fig. 2) and scaled up to the 10 cm settings the "effective" dispersion value would be around 18 cm at the screen location. Comparing it with the 0.42% rms energy spread this corresponds to 2.6 standard deviations of the bunch lasing or a total energy width of about 1.1%. Due to the quadratic nature of the FEL resonance equation the spectral width of the FEL pulse should be 2.2%, which agrees, within the limits of this rough estimate, with the observed 1.9% obtained from a monochromator scan at the user station.

Doubling the dispersion to 20 cm stretches the electron bunch transversely and reduces the electron density. With lower gain a smaller fraction of the bunch can reach saturation and the bandwidth of the FEL spectrum is narrowed down. Indeed, the observed extension of the FEL pulse on the YAG screen increases by only 500 μm, confirming the narrowing in the bandwidth. Since this was too narrow for the user experiment, and machine operation became rather unstable, the experiment was continued with the 10 cm dispersion settings.

The verification of the spatially tilted, frequency-chirped pulse was done at the Alvra user experimental station of SwissFEL. Here a silicon crystal, bent with a bending radius of 9.8 mm in the plane perpendicular to the tilted pulse, intercepts the FEL signal [15]. The (111) Bragg reflection deflects part of the FEL pulse upward. Since the central frequency varies with the transverse position, the varying Bragg angle yields a raw spectrometer image which is tilted on the screen as well. A raw image is presented in Fig. 5, showing spatial extension in the horizontal and photon energy in the vertical (dispersive) direction. The spectral axis was calibrated with monochromator scans.

The spectral resolution for a given spatial position is an important factor for the experiment at the user station and can be determined by the width of the distribution in the spectrometer image. Any vertical cut in the image determines the spectral purity, which for the example shown is on the order of a tenth of the total spectral width of 1.8% (full width). The resolution is limited by the intrinsic FEL mode size—the transverse size of the FEL pulse without energy and spatial chirps, compared to the spatial extent of the chirped FEL pulse. Under the assumption that the intrinsic mode has the same mode size in the two transverse dimensions, the ratio can also be derived from the distribution in the upper plot of Fig. 4. With a full width of about 200 μm in the vertical plane and little less than 2 mm in the horizontal, the ratio is about 10%, in agreement with the frequency resolution of the spectrometer. This reduced resolution is still sufficient for x-ray absorption spectroscopy without utilizing a monochromator. The resolution can further be improved by measuring the single shot spectrum (see Fig. 5) as the basis for a deconvolution algorithm. A description of the analysis of the obtained absorption spectra is beyond the scope of this Letter.

Several factors determine the resolution. The first is the intrinsic mode size. It must be considered unchangeable since changing it would require focusing of the electron beam, in contradiction with the need for a focusing-free beam transport along the undulator. Better control is obtained by increasing the chirp either in photon frequency or in the spatial domain. For the results presented here we were at the limit, since a larger dispersion causes unstable operation of the machine and the electron chirp was fixed by the compression scheme in the machine to yield best performance of the large bandwidth mode. The additional knob of a transverse gradient in the undulator field, which would increase the photon energy chirp independently from the electron chirp, is not available for Aramis (in contrast to the soft x-ray beamline Athos [27]).

In conclusion we have demonstrated a spatially tilted frequency-chirped FEL pulse, using the hard x-ray beamline Aramis at SwissFEL for our experiments. While the driving motivation was providing an FEL pulse for single-shot x-ray absorption spectroscopy without the need of dispersive elements in the optical beam line, this mode offers further opportunities, which we will briefly discuss in the remainder of this Letter.

In the given configuration of the dispersive section of the energy collimator, the nominal longitudinal dispersion R_{56} is small so that it has no significant impact on the electron bunch length. However, the flexibility of that beamline section allows

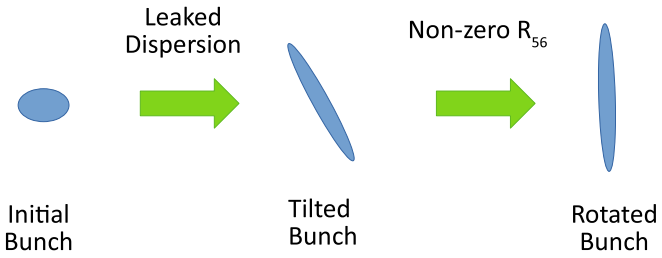

FIG. 6. Principle method for bunch rotation. A chirped beam is tilted with leaked dispersion and then compressed with a nonzero R_{56} setting of the energy collimator.

for independent control of the R_{56} parameter for adjustments of the final bunch length [40], while still leaking out dispersion for beam tilt generation.

Bunch rotation (see Fig. 6) as the combination of shearing (tilting) and compression opens the possibility to achieve shorter pulses beyond standard compression. The tolerable energy spread for the FEL process is given by the relation

$$\rho \geqslant \sigma_\delta, \tag{1}$$

where ρ is the FEL parameter [6] and σ_δ the relative rms energy spread of the electron beam. Since ρ scales as the cubic root of the peak current and the energy spread grows linearly with the current, it is evident that for certain bunch lengths the inequality of Eq. (1) gets violated. In particular for compact x-ray FEL facilities, operating at lower beam energies, this limit can easily be reached. The problem of increased energy spread as well as stronger longitudinal space charge fields [41] is mitigated by expanding the beam size transversely as in the case of the proposed bunch rotation. The larger transverse beam size can be partially compensated by a tighter focusing at the user station.

Bunch rotation still causes an increase of the intrinsic energy spread but significantly less than in conventional compression schemes based on magnetic chicanes. For instance, if the tilt extends 100 times the natural beam size within the undulator, only electrons within a range of about 1% of the original bunch length are mixed. Thus the degrading effect of Landau damping due to the intrinsic energy spread is mitigated, in contrast to conventional compression where the intrinsic energy spread grows linearly with the compression factor.

The advantage of shorter bunch lengths due to bunch rotation has to be weighed against the penalty of the FEL performance loss of about 50% when operating with a tilt and no focusing. Already a compression by a factor of two in the energy collimator would compensate this loss, recovering the photon flux of normal SASE operation but with a shorter pulse duration. This is effectively a form of x-ray pulse compression without the need of intercepting optical elements and would benefit any "diffract-before-destroy" setup for user experiments [42]. To further improve the signal for certain classes of user experiments, the photon energy chirp of the FEL pulse could be removed by compensating the broadening by the electron energy chirp with a matching transverse gradient of the undulator field. This is not possible for the hard x-ray beamline Aramis but an option to study for the soft x-ray beamline Athos at SwissFEL.

Another application of such a rotated bunch is the control of transverse coherence. For a constant value of the dispersion the transversely elongated bunch develops independent modes, separated in space analogous to the temporal spikes in normal SASE operation. If the dispersion function converges, the transverse momentum of the electron is transferred to these modes. At some location after the undulator these modes will overlap in a single point. Since these modes are not stacked behind each other but instead are emitted from the undulator side by side of each other from the fully compressed bunch, they will interfere, generating shot-to-shot fluctuations in the transverse profile in full analogy to the SASE spikes in time domain for normal SASE operation. Although such a setup reduces the degree of transverse coherence it can be useful if the normal SASE mode size is too large to exclude undesired diffraction between samples on a membrane or liquid media when their mean distance is smaller than the mode size [23]. With the slope of the dispersion function the degree of coherence can be controlled with only minor effect on other FEL parameters such as saturation power or saturation length.

We would like to thank T. Schietinger for carefully reading this manuscript and T. Mamyrbayev for helping in retrieving the data from the Alvra experimental station.

[1] P. Emma, R. Akre, J. Arthur, R. Bionta, C. Bostedt, J. Bozek, A. Brachmann, P. Bucksbaum, R. Coffee, F.-J. Decker, Y. Ding, D. Dowell, S. Edstrom, A. Fisher, J. Frisch, S. Gilevich, J. Hastings, G. Hays, P. Hering, Z. Huang *et al.*, First lasing and operation of an ångstrom-wavelength free-electron laser, Nat. Photon. **4**, 641 (2010).

[2] D. Pile, First light from SACLA, Nat. Photon. **5**, 456 (2011).

[3] H.-S. Kang, C.-K. Min, H. Heo, C. Kim, H. Yang, G. Kim, I. Nam, S. Y. Baek, H.-J. Choi, G. Mun, B. R. Park, Y. J. Suh, D. C. Shin, J. Hu, J. Hong, S. Jung, S.-H. Kim, K. Kim, D. Na, S. S. Park *et al.*, Hard X-ray free-electron laser with femtosecond-scale timing jitter, Nat. Photon. **11**, 708 (2017).

[4] W. Decking, S. Abeghyan, P. Abramian, A. Abramsky, A. Aguirre, C. Albrecht, P. Alou, M. Altarelli, P. Altmann, K. Amyan, V. Anashin, E. Apostolov, K. Appel, D. Auguste, V. Ayvazyan, S. Baark, F. Babies, N. Baboi, P. Bak, V. Balandin *et al.*, A MHz-repetition-rate hard X-ray free-electron laser driven by a superconducting linear accelerator, Nat. Photon. **14**, 391 (2020).

[5] E. Prat, R. Abela, M. Aiba, A. Alarcon, J. Alex, Y. Arbelo, C. Arrell, V. Arsov, C. Bacellar, C. Beard, P. Beaud, S. Bettoni, R. Biffiger, M. Bopp, H.-H. Braun, M. Calvi, A. Cassar, T. Celcer, M. Chergui, P. Chevtsov *et al.*, A compact and cost-effective hard X-ray free-electron laser driven by a high-brightness and low-energy electron beam, Nat. Photon. **14**, 748 (2020).

[6] R. Bonifacio, C. Pellegrini, and L. Narducci, Collective instabilities and high-gain regime in a free electron laser, Opt. Commun. **50**, 373 (1984).

[7] A. M. Kondratenko and E. L. Saldin, Generation of coherent radiation by a relaticistic electron beam in an ondulator, Part. Accel. **10**, 207 (1980).

[8] E. L. Saldin, E. A. Schneidmiller, and M. V. Yurkov, Statistical and coherence properties of radiation from x-ray free-electron lasers, New J. Phys. **12**, 035010 (2010).

[9] C. Dejoie, L. B. McCusker, C. Baerlocher, R. Abela, B. D. Patterson, M. Kunz, and N. Tamura, Using a non-monochromatic microbeam for serial snapshot crystallography, J. Appl. Crystallogr. **46**, 791 (2013).

[10] S. Baradaran, U. Bergmann, and H. Durr, LCLS-II New Instruments Workshops Report, Report No. SLAC-R-993 (2012), https://inspirehep.net/literature/1121052.

[11] J. Arthur, LCLS Ultrafast Science Instruments II (LUSI-II) Proposal, Report No. SLAC-R-8522013 (2007), https://inspirehep.net/literature/764476.

[12] K. Nass, R. Cheng, L. Vera, A. Mozzanica, S. Redford, D. Ozerov, S. Basu, D. James, G. Knopp, C. Cirelli, I. Martiel, C. Casadei, T. Weinert, P. Nogly, P. Skopintsev, I. Usov, F. Leonarski, T. Geng, M. Rappas, A. S. Doré *et al.*, Advances in long-wavelength native phasing at X-ray free-electron lasers, IUCrJ **7**, 965 (2020).

[13] B. D. Patterson, R. Abela, H.-H. Braun, U. Flechsig, R. Ganter, Y. Kim, E. Kirk, A. Oppelt, M. Pedrozzi, S. Reiche, L. Rivkin, T. Schmidt, B. Schmitt, V. N. Strocov, S. Tsujino, and A. F. Wrulich, Coherent science at the SwissFEL x-ray laser, New J. Phys. **12**, 035012 (2010).

[14] S.-K. Son, H. N. Chapman, and R. Santra, Multiwavelength Anomalous Diffraction at High X-Ray Intensity, Phys. Rev. Lett. **107**, 218102 (2011).

[15] P. Karvinen, S. Rutishauser, A. Mozzanica, D. Greiffenberg, P. N. Juranić, A. Menzel, A. Lutman, J. Krzywinski, D. M. Fritz, H. T. Lemke, M. Cammarata, and C. David, Single-shot analysis of hard x-ray laser radiation using a noninvasive grating spectrometer, Opt. Lett. **37**, 5073 (2012).

[16] D. Zhu, M. Cammarata, J. M. Feldkamp, D. M. Fritz, J. B. Hastings, S. Lee, H. T. Lemke, A. Robert, J. L. Turner, and Y. Feng, A single-shot transmissive spectrometer for hard x-ray free electron lasers, Appl. Phys. Lett. **101**, 034103 (2012).

[17] C. Milne, T. Schietinger, M. Aiba, A. Alarcon, J. Alex, A. Anghel, V. Arsov, C. Beard, P. Beaud, S. Bettoni, M. Bopp, H. Brands, M. Brönnimann, I. Brunnenkant, M. Calvi, A. Citterio, P. Craievich, M. Csatari Divall, M. Dällenbach, M. D'Amico *et al.*, SwissFEL: The Swiss X-ray Free Electron Laser, Appl. Sci. **7**, 720 (2017).

[18] S. Pascarelli, O. Mathon, M. Muñoz, T. Mairs, and J. Susini, Energy-dispersive absorption spectroscopy for hard-X-ray micro-XAS applications, J. Synchrotron Radiat. **13**, 351 (2006).

[19] S. Pascarelli, O. Mathon, T. Mairs, I. Kantor, G. Agostini, C. Strohm, S. Pasternak, F. Perrin, G. Berruyer, P. Chappelet, C. Clavel, and M. C. Dominguez, The Time-resolved and Extreme-conditions XAS (TEXAS) facility at the European Synchrotron Radiation Facility: The energy-dispersive X-ray absorption spectroscopy beamline ID24, J. Synchrotron Radiat. **23**, 353 (2016).

[20] T. Katayama, Y. Inubushi, Y. Obara, T. Sato, T. Togashi, K. Tono, T. Hatsui, T. Kameshima, A. Bhattacharya, Y. Ogi, N. Kurahashi, K. Misawa, T. Suzuki, and M. Yabashi, Femtosecond x-ray absorption spectroscopy with hard x-ray free electron laser, Appl. Phys. Lett. **103**, 131105 (2013).

[21] Y. Obara, T. Katayama, Y. Ogi, T. Suzuki, N. Kurahashi, S. Karashima, Y. Chiba, Y. Isokawa, T. Togashi, Y. Inubushi, M. Yabashi, T. Suzuki, and K. Misawa, Femtosecond time-resolved X-ray absorption spectroscopy of liquid using a hard X-ray free electron laser in a dual-beam dispersive detection method, Opt. Express **22**, 1105 (2014).

[22] J. Hrdý and P. Oberta, Possibility of X-ray pulse compression using an asymmetric or inclined double-crystal monochromator, J. Synchrotron Radiat. **20**, 550 (2013).

[23] S. Shin, K. Kim, K. Lee, S. Lee, and Y. Park, Effects of spatiotemporal coherence on interferometric microscopy, Opt. Express **25**, 8085 (2017).

[24] E. Prat, P. Dijkstal, E. Ferrari, and S. Reiche, Demonstration of Large Bandwidth Hard X-Ray Free-Electron Laser Pulses at SwissFEL, Phys. Rev. Lett. **124**, 074801 (2020).

[25] M. W. Guetg, B. Beutner, E. Prat, and S. Reiche, Optimization of free electron laser performance by dispersion-based beam-tilt correction, Phys. Rev. ST Accel. Beams **18**, 030701 (2015).

[26] E. Prat, M. Calvi, and S. Reiche, Generation of ultra-large-bandwidth X-ray free-electron-laser pulses with a transverse-gradient undulator, J. Synchrotron Radiat. **23**, 874 (2016).

[27] M. Calvi, C. Camenzuli, E. Prat, and T. Schmidt, Transverse gradient in Apple-type undulators, J. Synchrotron Radiat. **24**, 600 (2017).

[28] R. L. Gluckstern, Longitudinal impedance of a periodic structure at high frequency, Phys. Rev. D **39**, 2780 (1989).

[29] H. H. Braun, R. Corsini, L. Groening, F. Zhou, A. Kabel, T. O. Raubenheimer, R. Li, and T. Limberg, Emittance growth and energy loss due to coherent synchrotron radiation in a bunch compressor, Phys. Rev. ST Accel. Beams **3**, 124402 (2000).

[30] K. Bane and G. Stupakov, Dechirper wakefields for short bunches, Nucl. Instrum. Methods Phys. Res., A **820**, 156 (2016).

[31] P. Emma and Z. Huang, Femtosecond X-ray pulses from a spatially chirped electron bunch in a SASE FEL, Nucl. Instrum. Methods Phys. Res., A **528**, 458 (2004), Proceedings of the 25th International Free Electron Laser Conference, and the 10th FEL Users Workshop.

[32] Y. Ding, C. Behrens, P. Emma, J. Frisch, Z. Huang, H. Loos, P. Krejcik, and M.-H. Wang, Femtosecond x-ray pulse temporal characterization in free-electron lasers using a transverse deflector, Phys. Rev. ST Accel. Beams **14**, 120701 (2011).

[33] A. A. Lutman, T. J. Maxwell, J. P. MacArthur, M. W. Guetg, N. Berrah, R. N. Coffee, Y. Ding, Z. Huang, A. Marinelli, S. Moeller, and J. C. U. Zemella, Fresh-slice multicolour X-ray free-electron lasers, Nat. Photon. **10**, 745 (2016).

[34] P. Dijkstal, A. Malyzhenkov, S. Reiche, and E. Prat, Demonstration of two-color x-ray free-electron laser pulses with a sextupole magnet, Phys. Rev. Accel. Beams **23**, 030703 (2020).

[35] K. Bane, G. Stupakov, and I. Zagorodnov, Analytical formulas for short bunch wakes in a flat dechirper, Phys. Rev. Accel. Beams **19**, 084401 (2016).

[36] S. Reiche, GENESIS 1.3: A fully 3D time-dependent FEL simulation code, Nucl. Instrum. Methods Phys. Res., A **429**, 243 (1999).

[37] Z. Huang, Y. Ding, and C. B. Schroeder, Compact X-ray Free-Electron Laser from a Laser-Plasma Accelerator Using a Transverse-Gradient Undulator, Phys. Rev. Lett. **109**, 204801 (2012).

[38] M. Calvi, C. Camenzuli, R. Ganter, N. Sammut, and T. Schmidt, Magnetic assessment and modelling of the Aramis undulator beamline, J. Synchrotron Radiat. **25**, 686 (2018).

[39] E. Scharlemann, Wiggle plane focusing in linear wigglers, J. Appl. Phys. **58**, 2154 (1985).

[40] Á. Saá Hernández, E. Prat, and S. Reiche, Generation of two-color x-ray free-electron-laser pulses from a beam with a large energy chirp and a slotted foil, Phys. Rev. Accel. Beams **22**, 030702 (2019).

[41] G. Geloni, E. Saldin, E. Schneidmiller, and M. Yurkov, Longitudinal impedance and wake from XFEL undulators. Impact on current-enhanced SASE schemes, Nucl. Instrum. Methods Phys. Res., A **583**, 228 (2007).

[42] H. N. Chapman, P. Fromme, A. Barty, T. A. White, R. A. Kirian, A. Aquila, M. S. Hunter, J. Schulz, D. P. DePonte, U. Weierstall, R. B. Doak, F. R. N. C. Maia, A. V. Martin, I. Schlichting, L. Lomb, N. Coppola, R. L. Shoeman, S. W. Epp, R. Hartmann, D. Rolles *et al.*, Femtosecond X-ray protein nanocrystallography, Nature (London) **470**, 73 (2011).